Destruction of pancreatic β-cells by transgenic induction of prostaglandin e2 in the islets

DESTRUCTION OF PANCREATIC β-CELLS BY TRANSGENIC INDUCTION OF PROSTAGLANDIN E_2 IN THE ISLETS*

Hiroko Oshima[1,2], Makoto Mark Taketo[2], & Masanobu Oshima[1,2]

From the [1]Division of Genetics, Cancer Research Institute, Kanazawa University, Kanazawa 920-0934, Japan; and [2]Department of Pharmacology, Kyoto University Graduate School of Medicine, Kyoto 606-8501, Japan

Running Title: Pancreatic β-Cell Destruction by PGE_2 Signaling

Address correspondence to: Masanobu Oshima, Division of Genetics, Cancer Research Institute, Kanazawa University, 13-1 Takara-machi, Kanazawa 920-0934, Japan, Tel. 81-76-165-2721; Fax. 81-76-234-4519; E-Mail: oshimam@kenroku.kanazawa-u.ac.jp

Type 2 diabetes mellitus is characterized by insulin resistance of peripheral tissues and dysfunction of pancreatic β-cells. Furthermore, the number of pancreatic β-cells decreases as a secondary effect of advanced type 2 diabetes, although molecular mechanism has not been elucidated. Recently, it has been shown that hyperglycemic conditions induce the expression of cyclooxygenase-2 (COX-2) in pancreatic islets and increase the downstream product prostaglandin E_2 (PGE_2). To investigate whether high glucose-induced PGE_2 has an adverse effect on pancreatic β-cells, we generated transgenic mice (*RIP-C2mE*) that express COX-2 and microsomal prostaglandin E synthase-1 (mPGES-1) in their β-cells using the rat insulin-2 gene promoter (RIP). The homozygous *RIP-C2mE* (*Tg*/*Tg*) mice showed severe hyperglycemia from 6 weeks of age. Although the heterozygous *RIP-C2mE* (*Tg*/–) mice showed normal blood glucose levels throughout their lifetime, this level increased significantly compared with that of wild-type mice when glucose was loaded. The relative number of β-cells to the total islet cell number was reduced to 54% and 14% in the *RIP-C2mE* (*Tg*/–) and (*Tg*/*Tg*) mice, respectively, whereas that in the wild-type mice was 84%. Importantly, the proliferation rate in the islets of the *RIP-C2mE* (*Tg*/*Tg*) mice at four weeks of age decreased significantly in comparison to that in the wild-type mice. Because β-cells replicate not only during the postnatal period but also in the adult pancreas at a basal level, it is possible that increased PGE_2 signaling thus contributes to the reduction of the pancreatic β-cell mass through inhibition of proliferation, thereby aggravating diabetes further.

Type 2 diabetes mellitus is characterized by the insensitivity of the peripheral tissues to insulin and the reduced function of the pancreatic β-cells. It has been suggested that chronic hyperglycemia impairs β-cell function as a secondary adverse effect of diabetes (1). Furthermore, the β-cell mass in pancreatic islets is reduced significantly in type 2 diabetes patients (2,3,4). In type 1 diabetes, a complexed autoimmune disease, an inflammatory cytokine IL-1β is an important

mediator in the impaired function and destruction of pancreatic β-cells (5). For example, the treatment of isolated islets with IL-1 inhibits insulin secretion, and this is followed by islet destruction (6). Moreover, adenoviral transduction of the IL-1 receptor antagonist protein into the islets protects against the IL-1β-induced dysfunction (7). On the other hand, the long-term exposure of islets to high glucose conditions has been shown to result in the induction of IL-1β, followed by β-cell apoptosis (8). This high glucose-induced β-cell destruction is prevented by treating the islets with an IL-1 receptor antagonist. Accordingly, it is possible that IL-1β plays a pivotal role in type 2 diabetes as well.

Recently, it has been reported that high glucose conditions induce the expression of cyclooxygenase-2 (COX-2) in pancreatic islets with an increase of the downstream product prostaglandin E_2 (PGE_2) (9,10). COX-2 expression has also been detected in the pancreatic islets of *db*/*db* mice, a mouse model for type 2 diabetes mellitus (10). COX-2 is a rate-limiting enzyme for prostanoid biosynthesis and plays various roles in physiological and pathological conditions such as reproduction, inflammation and tumorigenesis (11). Although conflicting results have been reported, several studies indicate that the COX-2 pathway contributes to the pathogenesis of type 1 diabetes. For example, IL-1β – a cytokine responsible for type 1 diabetes – induces COX-2 expression and PGE_2 production in pancreatic islets (12). IL-1β-induced β-cell dysfunction is suppressed by the treatment of the islets with COX-2 inhibitors (13). Moreover, the destruction of the pancreatic β-cells in streptozotocin (STZ)-treated mice was inhibited by treatment with a COX-2 selective inhibitor, NS-398 (14). Therefore, it is possible that the hyperglycemia-induced production of IL-1β in the islets of type 2 diabetes causes the dysfunction and destruction of β-cells through further induction of the COX-2 pathway.

In order to investigate the genetic mechanism of PGE_2 signaling in pancreatic islets, we constructed transgenic mice that expressed COX-2 and microsomal prostaglandin E synthase-1 (mPGES-1) in their pancreatic β-cells by using the rat insulin-2 gene promoter (RIP). The inducible enzyme mPGES-1 catalyzes the conversion of PGH_2 to PGE_2, and appears to be functionally coupled with COX-2 (15). In this study, we provide genetic evidence that increased PGE_2 signaling causes the decrease of pancreatic β-cells in a dose-dependent manner.

Experimental Procedures

Transgenic Mice – The RIP fragment (704 bp; nucleotide position, -695 to +8 of the rat insulin-2 gene) was amplified by PCR using rat genomic DNA and the following primers: 5′-GGGATCCCCCAACCACT-3′ and 5′-TTAGGGCTGGGGGTTACTGAA-3′. After confirming the nucleotide sequences, the RIP fragment was subcloned into both expression vectors of COX-2 and mPGES-1 at the 5′ position in the same orientation as that of cDNAs. Both expression vectors contained RIP, a synthetic chimeric intron excised from pCI (Promega, La Jolla, CA), cDNA for mouse COX-2 or mPGES-1, and a SV40 poly(A)

cassette (Fig. 1*A*). Mouse COX-2 and mPGES-1 cDNAs were cloned by RT-PCR as previously described (16). The transcription unit was excised from each expression vector, purified, and co-microinjected into fertilized eggs from a cross between F_1 (C3H and C57BL/6) hybrid females and C57BL/6 males. We obtained 14 founder mice that carried both the COX-2 and mPGES-1 transgenes. Among the F1 progenies of these 14 lines, two lines (*RIP-C2mE* #8 and *RIP-C2mE* #9) showed high amounts of both COX-2 and mPGES-1 mRNAs in their pancreatic tissues. These two transgenic lines showed essentially the same phenotypes. N2-backcrossed transgenic mice with C57BL/6 were intercrossed to generate homozygous *RIP-C2mE* (*Tg*/*Tg*) and heterozygous *RIP-C2mE* (*Tg*/–) mice. Backcrossing was performed using wild-type C57BL/6 mice. Mice of the N2F1 generation were used for the experiments. Littermate wild-type mice were used as controls for the experiments. Genotyping was performed by genomic PCR using tail DNA and the following primer sets: COX-2, 5′-CAAACTCAAGTTTGACCCAG-3′ and 5′-GCCGGGATCCTTTTACAGCTCAGTTGAACG-3′; mPGES-1, 5′-CCGAATTCTTGAAGTCCAGGCCGGCTAG-3′ and 5′-GTCAGCAGTAGCCTCATCATCACT-3′. Homozygotes were identified by increased band intensities of the genomic PCR products in comparison to those of the heterozygotes.

Pancreatic Islet Isolation – Pancreata injected with 0.2% Collagenase Type I (Invitrogen, Carlsbad, CA) in Hank's buffered saline solution via the bile duct were collected and incubated for 20 min at 37^0C. After digestion, islets were then hand picked using a dissecting microscope.

RT-PCR – Total RNA was extracted from the isolated islets using ISOGEN (Nippon Gene, Tokyo, Japan). The extracted RNA was reverse transcribed and PCR amplified. The primer sets used for genotyping were also used for RT-PCR analyses of COX-2 and mPGES-1. GAPDH was used as an internal control.

Measurement of Pancreatic PGE_2 Level – The PGE_2 levels were measured at SRL (SRL Inc., Tokyo, Japan) using 6 *RIP-C2mE* (*Tg*/–) and 6 wild-type mice at 20 weeks of age, and 4 *RIP-C2mE* (*Tg*/–) and 4 *RIP-C2mE* (*Tg*/ *Tg*) mice at 3 weeks of age. Briefly, the pancreata were homogenized in a lysis buffer, and PGE_2 was extracted with ethanol. The PGE_2 levels were measured using Prostaglandin E_2 [^{125}I] RIA Kit (Perking Elmer Life Science, Boston, MA). According to the manufacturer's instruction manual, the cross reactivity of this kit is as follows: PGE_2 (100%), $PGF_{2\alpha}$ (0.9%), PGD_2 (0.3%), 6-keto-$PGF_{1\alpha}$ (1%) and thromboxane B_2 (0.01%). The islet PGE_2 levels of the *RIP-C2mE* (*Tg*/ *Tg*) mice relative to (*Tg*/–) mice at 3 weeks of age was calculated using the ratio of the islet area in the pancreas. To determine the ratio of the islet area in the *RIP-C2mE* (*Tg*/–) and (*Tg*/ *Tg*) mice, five sections per pancreas of each genotype were scanned using an ImageJ program (NIH) and then the islet area was quantified versus the total pancreas area.

Measurement of Blood Glucose, Plasma Insulin, and Plasma Glucagon Levels – The blood glucose levels were measured using Glutest AceR (Sanwa Chemical, Nagoya, Japan). For

chronological observation, the blood glucose level was examined when the mice were 3, 6, 9, and 12 weeks of age. In this experiment, 6 wild-type, 12 *RIP-C2mE* (*Tg*/−), and 11 *RIP-C2mE* (*Tg*/*Tg*) mice were used. The plasma insulin levels were examined through use of the High-Sensitive Insulin Measurement Kit that is based on an ELISA test (Morinaga, Yokohama, Japan) at 0 and 20 min of the glucose tolerance test. The plasma glucagon levels were measured by a radioimmunoassay which uses the Glucagon Kit Daiichi II at SRL (Tokyo, Japan), with 10 wild-type and 4 *RIP-C2mE* (*Tg*/*Tg*) mice.

Glucose Tolerance Test – The mice were fasted for 14 hours following an *i.p.* injection of glucose (1 g/kg body weight). Blood samples were obtained from a tail vein at 10, 20, 30, 60, and 120 min after the glucose injection. The blood glucose and plasma insulin levels were measured as described. In the glucose tolerance test, 7 wild-type and 8 *RIP-C2mE* (*Tg*/−) mice at 50 weeks of age were used.

Histopathology and Immunohistochemistry – Pancreatic tissues of the mice were fixed in 4% paraformaldehyde, embedded, and sectioned at a 4 μm-thickness. These sections were stained with H & E and were processed further for immunostaining. Rabbit polyclonal antibody for insulin (Progen Biotechnik, Heidelberg, Germany) and sheep polyclonal antibody for glucagon (Biogenesis, England, UK) were used as the primary antibody for an immunohistochemistry to detect β-cells and α cells, respectively. Rat monoclonal antibodies for CD3ε (BD, Franklin Lakes, NJ), F4/80 (Serotec, Oxford, UK) and Gr-1/Ly-6G (BD, San Jose, CA) were used as the primary antibodies to detect T cells, macrophages and neutrophils, respectively. Staining signals were visualized using the Vectorstain Elite kit (Vector, Burlingame, CA). Alexa Fluor 594 donkey anti-sheep IgG or Alexa Fluor 488 donkey anti-rabbit IgG (Molecular Probes, Eugene, OR) was used as the secondary antibody.

Apoptosis Analysis – The pancreatic tissues of the mice at 4 weeks of age were fixed in 4% paraformaldehyde, embedded, and sectioned at a 4 μm-thickness. Apoptosis was determined based upon the TUNEL method, which uses the ApopTag Peroxidase in situ Apoptosis Detection Kit (Chemicon, Temecula, CA) according to the manufacturer's protocol.

Cell Proliferation Analysis – Mice were injected *i.p.* with 1 ml of a BrdU solution (1 mg/ml). At 3 hours post-injection, pancreatic tissues were fixed in 4% paraformaldehyde, embedded, and sectioned at a 4 μm-thickness. The sections were immunostained with an anti-BrdU antibody using the BrdU *In-Situ* Detection Kit (BD, San Jose, CA). The number of BrdU-labeled cells and total number of islet cells were scored from 10 islets and a mean BrdU labeling index was calculated.

Scoring the Ratio of α-Cells and β-Cells in the Pancreatic Islets – At least 6 nonoverlapping fields of the fluorescence-immunostained sections were photographed (total number of islets > 12), and the number of glucagon-positive α-cells and insulin-positive β-cells were scored. The ratio of α-cells and β-cells in the islet was calculated by dividing each number with the total number of islet cells. The total cell number in each islet was scored using the same sections under a differential

interference microscope, DM5000B (Leica Microsystems, Wetzler, Germany).

Statistical Analysis – Statistical analyses were carried out using the unpaired Student's *t* test, and a *P* value of < 0.05 was considered to be significant.

RESULTS

In order to investigate the effects of PGE_2 on the pancreatic β-cells in mice, we generated transgenic (*RIP-C2mE*) mice expressing both COX-2 and mPGES-1 by co-microinjection of the two expression vectors (Fig. 1*A*). We used RIP to target the β-cells in the pancreatic islets. To increase the expression level of the transgenes, we introduced a synthetic intron between the RIP and cDNAs for COX-2 and mPGES-1 (16). Two transgenic lines (*RIP-C2mE*#8 and *RIP-C2mE*#9) essentially exhibited the same phenotype (data not shown). Accordingly, we present the results with *RIP-C2mE*#8 (hereafter referred to as *RIP-C2mE*). We detected high amounts of mRNA of COX-2 and mPGES-1 by RT-PCR in the isolated islets from the *RIP-C2mE* (*Tg*/–) mice, while the expression of both genes was found in the wild-type islets at a basal level (Fig. 1*B*). We consistently found strong immunostaining signals for COX-2 and mPGES-1 in the pancreatic islets of the *RIP-C2mE* (*Tg*/–) mice compared with those of the wild-type mice (Fig. 1*C*). As shown in Fig. 1*D*, pancreatic PGE_2 levels at 20 weeks of age increased significantly in the *RIP-C2mE* (*Tg*/–) mice (10.9 ± 2.2 pg/mg) in comparison to that in the wild-type mice (4.2 ± 0.5 pg/mg), indicating that the simultaneous transgenic expression of COX-2 and mPGES-1 produced PGE_2 *in vivo*.

The blood glucose level in the *RIP-C2mE* (*Tg*/–) mice did not differ from that in the wild-type mice at 4 months of age (data not shown). To examine whether increased PGE_2 affects β-cell function under hyperglycemic conditions, we carried out the glucose tolerance test using fasted *RIP-C2mE* (*Tg*/–) mice. As shown in Fig. 2*A*, the *RIP-C2mE* (*Tg*/–) mice showed a significant increase in the blood glucose level in comparison to that in the wild-type mice from 10 to 60 min after the glucose injection. In the wild-type mice, the plasma insulin level at 20 min post-glucose injection increased significantly in comparison to that at 0 min (Fig. 2*B*). However, the plasma insulin level in the *RIP-C2mE* (*Tg*/–) mice at 20 min was significantly lower than that in the wild-type mice, although it had increased a 1.3 fold of the basal level at 0 min. These results indicate that increased PGE_2 in the pancreatic β-cells causes impaired insulin secretion under hyperglycemic conditions.

To further investigate the role of PGE_2 signaling in pancreatic β-cells, we intercrossed heterozygous *RIP-C2mE* (*Tg*/–) mice to generate homozygous *RIP-C2mE* (*Tg*/*Tg*) mice that carried double the copy number of each transgene. The mean PGE_2 level in the pancreas of the *RIP-C2mE* (*Tg*/*Tg*) mouse at 3 weeks of age was higher than that in the pancreas of the *RIP-C2mE* (*Tg*/–) mice, although it was not significant (Fig. 3*A*). However, the ratio of islet area in the pancreas of the *RIP-C2mE* (*Tg*/*Tg*) mice was lower than that in the *RIP-C2mE* (*Tg*/–) mice (0.39% and 0.59% of the total pancreas in the *Tg*/*Tg* and

Tg/− mice, respectively). Consequently, the relative islet PGE_2 level in the *RIP-C2mE* (*Tg*/*Tg*) mice was a 1.9-fold higher than that in the *RIP-C2mE* (*Tg*/−) mice (Fig. 3*B*). We determined the blood glucose level chronologically when the mice were 3, 6, 9, and 12 weeks of age (Fig. 3*C*). The blood glucose levels in the *RIP-C2mE* (*Tg*/−) mice were normal at all examined ages; this was consistent with the results of the blood glucose tolerance test. However, the homozygous *RIP-C2mE* (*Tg*/*Tg*) mice showed a significant increase in the blood glucose levels from 6 weeks of age, thus suggesting that insulin secretion was inhibited by PGE_2 signaling in a dose-dependent manner. Importantly, the blood glucose level of the *RIP-C2mE* (*Tg*/*Tg*) mice at 3 weeks of age was at the normal level, indicating that the dysfunction of the pancreatic β-cells was not caused by the congenital anomaly of the pancreatic islets.

We then examined the pancreatic β-cells by fluorescence immunohistochemistry using pancreatic tissue of the respective mouse genotypes at 16 weeks of age. In the wild-type mice, the insulin-positive β-cells predominated the pancreatic islets, whereas the glucagon-producing α-cells were found scattered in the marginal regions of the islets (Fig. 4*A*). In the heterozygous *RIP-C2mE* (*Tg*/−) mice, the number of β-cells decreased compared with that in the wild-type mice, while the α-cell population increased slightly (Fig. 4*B*). In sharp contrast to the wild-type mice, α-cells predominated the *RIP-C2mE* (*Tg/Tg*) mouse islets, and the β-cells were sparsely distributed in the center of the islets (Fig. 4*C*). The mean relative ratio of β-cells to the total number of islet cells was 84%, 54%, and 14% in the wild-type, *RIP-C2mE* (*Tg*/−), and (*Tg/Tg*) mice, respectively (Fig. 4*D*). In contrast, the mean ratio of α-cells increased inversely with the *RIP-C2mE* (*Tg*/−) and (*Tg/Tg*) mice (Fig. 4*E*). However, the mean plasma glucagon level in the *RIP-C2mE* (*Tg/Tg*) mice stayed at similar level to that found in the wild-type mice (97.0 ± 4.4 pg/ml and 101.3 ± 9.2 pg/ml in the wild-type and *RIP-C2mE* (*Tg*/*Tg*) mice, respectively). These results collectively indicate that an increase in the PGE_2 level causes a diabetic phenotype through a decrease in the number of pancreatic β-cells.

In order to rule out the possibility that PGE_2 signaling impairs the development of the pancreatic islets, we carried out fluorescence immunohistochemistry with mice at 3 weeks of age. The number of pancreatic β-cells in the wild-type mice at 3 weeks of age was less than that found at 16 weeks of age (Fig. 5*A* and *C*; and Fig. 4*A* and *D*). It is possible that the number of β-cells is still increasing at 3 weeks of age because β-cells replicate during the postnatal period to increase the β-cell mass to that of an adult level (17). Notably, the number of β-cells in the homozygous *RIP-C2mE* (*Tg/Tg*) mice was at the same level as that in the wild-type mice (Fig. 5*B* and *C*). Consistently, the number of α-cells in the *RIP-C2mE* (*Tg/Tg*) mice also demonstrated the same level as that of the wild-type mice (Fig. 5*D*). These results, taken together, indicate that increased PGE_2 signaling causes a decrease in the number of β-cells after weaning.

To further investigate the mechanism of β-cell destruction, we examined apoptosis in the pancreatic islets at 4 weeks of age by the

TUNEL method. However, we did not find any apoptotic cells in the islets of the *RIP-C2mE* (*Tg*/*Tg*) mice or the wild-type mice (data not shown). We thus examined the cell proliferation rate by BrdU incorporation at 4 weeks of age. Although the proliferation rate in the islets of the *RIP-C2mE* (*Tg*/–) mice was almost the same as that in the wild-type mice (Fig. 5*E*, *F* and *H*), it was decreased significantly in the *RIP-C2mE* (*Tg*/*Tg*) mice (Fig. 5*G* and *H*), thus suggesting that PGE_2 signaling inhibits the proliferation of β-cells.

It has been suggested that the COX-2 pathway is involved in the development of the autoimmune disease, type 1 diabetes (12,13,14). It was thus possible that the increased PGE_2 signaling had induced a host inflammatory or immune response in the pancreatic islets, thus causing further β-cell destruction. To assess this possibility, we histologically examined the islets of the homozygous *RIP-C2mE* (*Tg/Tg*) mice. Although the islets of the (*Tg/Tg*) mice appeared to be smaller than those of the wild-type mice, no inflammatory cell infiltration was observed around either of the islets in the *RIP-C2mE* (*Tg/Tg*) and wild-type mice (Fig. 6*A* and *B*). Furthermore, we did not find any infiltration of T lymphocytes (CD3), macrophages (F4/80) or neutrophils (Gr-1) around islets of the *RIP-C2mE* (*Tg/Tg*) mice at both 4 and 16 weeks of age (Fig. 6*C*, *D*, *E*, and *F*). Therefore, these results indicate that an inflammatory or immune response is not involved in the PGE_2-induced destruction of pancreatic β-cells.

DISCUSSION

In advanced type 2 diabetes mellitus, the pancreatic β-cell mass reduces through oxidative stress-related damage or increased apoptosis, resulting in secondary adverse effects upon β-cells (2,3,4). It has been demonstrated that hyperglycemic conditions induce the IL-1β, which is responsible for the dysfunction and destruction of pancreatic β-cells (8). Recently, it has been shown that COX-2 expression is also induced in the pancreatic islets under high glucose conditions (9,10). Moreover, IL-1β signaling stimulates COX-2 induction and PGE_2 production in pancreatic islets (12,13,18). These results, taken together, suggest that COX-2 plays a role in the IL-1β-induced β-cell damage. Here, we demonstrate that the expression of COX-2 and mPGES-1, which leads to an increase in islet PGE_2 production, causes a significant decrease in the number of pancreatic β-cells. These results provide the first genetic evidence for the causal role of the COX-2/PGE_2 pathway in β-cell destruction. Importantly, after doubling the number of copies of COX-2 and mPGES-1 by generating homozygous *RIP-C2mE* (*Tg/Tg*) mice, there was severe reduction of the β-cell mass with a significant increase in the blood glucose level when compared with the heterozygous *RIP-C2mE* (*Tg*/–) mice. Therefore, it is possible that the induction level of COX-2 and PGE_2 is correlated with the severity of the pancreatic β-cell damage in type 2 diabetes.

Although the number of α-cells was elevated in the adult *RIP-C2mE* (*Tg/Tg*) mice, the plasma glucagon level was not increased. Thus, increased blood glucose is caused by the reduced number of β-cells and not by the increased number of α-cells. We herein found a

significant decrease in the cell proliferation rate in the *RIP-C2mE* (*Tg*/*Tg*) mouse islets at 4 weeks of age. Because β-cells replicate during the postnatal period (17), it is possible that these proliferating cells are β-cells, and that PGE_2 signaling inhibits this β-cell proliferation. The number of β-cells in the normal adult islets is regulated by a balance between proliferation and apoptosis (19). It has been estimated that it takes 3 months for the renewal of 50% of the pancreatic β-cells (20) and 9 months for the renewal of 98% (21). Accordingly, it is conceivable that increased PGE_2 signaling suppresses β-cell proliferation in the adult islets, resulting in gradual reduction of the β-cell mass.

Recently, it has been demonstrated that the expression of $p27^{Kip1}$ plays a key role in regulation of the pancreatic β-cell mass, and that deletion of the gene encoding $p27^{Kip1}$ in the type 2 diabetes model (*db*/*db* mice) prevents β-cell destruction (22). Therefore, it is important to investigate the underlying relationship between PGE_2 and $p27^{Kip1}$ in β-cell destruction.

Type 1 diabetes mellitus is characterized by β-cell destruction due to autoimmune responses, which are critically dependent upon the interaction between antigen-presenting cells and T cells. Because we did not observe inflammatory or immune cell infiltration around the pancreatic islets in the *RIP-C2mE* mice, we concluded that the inhibition of β-cell proliferation in our mouse model is not caused by host immune responses. However, IL-1β signaling also plays an important role in the β-cell destruction of type 1 diabetes (23). Furthermore, the IL-1β-induced inhibition of insulin secretion is suppressed by COX-2 inhibitors; this is reconfirmed by exogenous PGE_2 stimulation (13). Therefore, it is possible that PGE_2 plays some role as a downstream mediator of the IL-1β pathway during β-cell destruction in type 1 diabetes as well.

It has been suggested that chronic inflammation plays an etiological role in type 2 diabetes (24), and that chronic activation of the immune system causes a decrease in insulin sensitivity, which may contribute to the pathogenesis of type 2 diabetes (25). The present results suggest that chronic inflammatory responses are involved in the decrease of pancreatic β-cells via the induction of COX-2 and PGE_2, which leads to an increased susceptibility to type 2 diabetes. Moreover, an epidemiological study has indicated the association of the promoter variant of the COX-2 gene with type 2 diabetes in Pima Indians (26). Although COX-2 is an inducible enzyme in most tissues, it has shown to be expressed constitutively in pancreatic islets (27). Therefore, it is probable that an increase in the basal level of COX-2 expression, caused by a promoter polymorphism, enhances the susceptibility to type 2 diabetes via the suppression of the renewing capabilities of islet β-cells. It is therefore possible that the blockade of PGE_2 receptors or the inhibition of mPGES-1 is an effective therapeutic strategy against β-cell destruction in type 2 as well as type 1 diabetes mellitus.

REFERENCES

1. Unger, R. H., and Grundy, S. (1985) *Diabetologia* **28**, 119-121
2. Sakuraba, H., Mizukami, H., Yagihashi, N., Wada, R., Hanyu, C., and Yagihashi, S. (2002) *Diabetrogia* **45**, 85-96
3. Butler, A. E., Janson, J., Bonner-Weir, S., Ritzel, R., Rizza, R. A., and Butler, P. C. (2003) *Diabetes* **52**, 102-110
4. Deng, S., Vatamaniuk, M., Huang, X., Doliba, N., Lian, M.-M., Frank, A., Velidedeoglu, E., Desai, N. M., Koeberlein, B., Wolf, B., Barker, C. F., Naji, A., Matschinsky, F. M., and Markmann, J. F. (2004) *Diabetes* **53**, 624-632
5. Mandrup-Poulsen, T. (1996) *Diabetologia* **39**, 1005-1029
6. Bendtzen, K., Mandrup-Poulsen, T., Nerup, J., Nielsen, J. H., Dinarello, C. A., and Svenson, M. (1986) *Science* **232**, 1545-1547
7. Giannoukakis, N., Rudert, W. A., Ghivizzani, S. C., Gambotto, A., Ricordi, C., Trucco, M., and Robbins, P. D. (1999) *Diabetes* **48**, 1730-1736.
8. Maedler, K., Sergeev, P., Ris, F., Oberholzer, J., Joller-Jemelka, H. I., Spinas, G. A., Kaiser, N., Halban, P. A., and Donath, M. Y. (2002) *J. Clin. Invest.* **110**, 851-860
9. Persaud, S. J., Burns, C. J., Belin, V. D., and Jones, P. M. (2004) *Diabetes* **53**, S190-S192
10. Shanmugam, N., Todorov, I. T., Nair, I., Omori, K., Reddy, M. A., and Natarajan, R. (2006) *Diabetologia* **49**, 100-107
11. DuBois, R. N., Abramson, S. B., Crofford, L., Gupta, R. A., Simon, L. S., Van de Putte, L. B. A., and Lipsky, P. E. (1998) *FASEB J*. **12**, 1063-1073
12. Sorli, C. H., Zhang, J.-J., Armstrong, M. B., Rajotte, R. V., Maclouf, J., and Robertson, R. P. (1998) *Proc. Natl. Acad. Sci. USA* **95**, 1788-1793
13. Tran, P. O., Gleason, C. E., Poitout, V., and Robertson, R. P. (1999) *J Biol Chem* **274**, 31245-31248
14. Tabatabaie, T., Waldon, A. M., Jacob, J. M., Floyd, R. A., and Kotake, Y. (2000) *Biochem. Biophys. Res. Commun*. **273**, 699-704
15. Murakami, M., Naraba, H., Tanioka, T., Semmyo, N., Nakatani, Y., Kojima, F., Ikeda, T., Fueki, M., Ueno, A., Oh-ishi, S., and Kudo, I. (2000) *J. Biol. Chem*. **275**: 32783-32792
16. Oshima, H., Oshima, M., Inaba, K., and Taketo, M. M. (2004) *EMBO J.* **23**, 1669-1678
17. Svenstrup, K., Skau, M., Pakkenberg, B., Buschard, K., and Bock, T. (2002) *APMIS* **110**, 372-378
18. Corbett, J. A., Kwon, G., Turk, J., and McDaniel, M. L. (1993) *Biochemistry* **32**, 13767-13770
19. Lingohr, M. K., Buettner, R., and Rhodes, C. J. (2002) *Trends Mol. Med.* **8**, 375-384.
20. Finegood, D. T., Scaglia, I., and Bonner-Weir, S. (1995) *Diabetes* **44**, 249-256
21. Dor, Y., Brown, J., Martinez, O. I., and Melton, D. A. (2004) *Nature* **429**, 41-46
22. Uchida, T., Nakamura, T., Hashimoto, N., Matsuda, T., Kotani, K., Sakaue, H., Kido, Y., Hayashi, Y., Nakawama, K., White, M. F., and Kasuga, M. (2005) *Nat Med* **11**, 175-182
23. Mandrup-Poulsen, T. (2003) *Ann. N.Y. Acad. Sci.* **1005**, 32-42

24. Schmidt, M. I., Duncan, B. B., Sharrett, A. R., Lindberg, G., and Savage, P. J., Offenbacher, S., Azambuja, M. I., Tracy, R. P., and Heiss, G. (1999) *Lancet* **353**, 1649-1652
25. Vozarova, B., Weyer, C., Lindsay, R. S., Pratley, R. E., Bogardus, C., and Tataranni, P. A. (2002) *Diabetes* **51**, 455-461
26. Konheim, Y. L., and Wolford, J. K. (2003) *Hum. Genet.* **113**, 377-381
27. Robertson, R. P. (1998) *Diabetes* **47**, 1379-1383

FOOTNOTE

*We thank Manami Watanabe, Akiko Kuwabara, and Asako Nakamura for their technical assistance and Nobuya Inagaki for discussions. This work was supported by Grant-in-Aid for Scientific Research from the Ministry of Education, Culture, Sports, Science and Technology of Japan, and Takeda Science Foundation.

Abbreviations used are: COX-2, cyclooxygenase-2; PGE_2, prostaglandin E_2; RIP, rat insulin-2 promoter; mPGES-1, microsomal prostaglandin E synthase-1; STZ. streptozotocin.

FIGURE LEGENDS

Fig. 1. Generation of *RIP-C2mE* transgenic mice. *A*, Schematic construction of transgenic vectors for COX-2 (*top*) and mPGES-1 (*bottom*). The synthetic chimeric intron is indicated by a V shape between the RIP and each cDNA fragment. COX-2 and mPGES-1 cDNA fragments and SV40 poly(A) cassettes are indicated as gray and black boxes, respectively. *B*, Representative RT-PCR for COX-2, mPGES-1 and GAPDH using the RNA prepared from isolated islets. *Tg*, *RIP-C2mE* (*Tg*/–) mice; *W*, wild-type mice; *M*, molecular weight marker (λ DNA digested with *Eco*RI/*Hind*III). *C*, Representative immunohistochemistry for COX-2 (*top*) and mPGES-1 (*bottom*) in the pancreatic islets of the wild-type (*left*) and *RIP-C2mE* (*Tg*/–) mice (*right*). Bars, 100 μm. *D*, The PGE_2 levels compared to the total pancreatic weight are indicated for the wild-type and *RIP-C2mE* (*Tg*/–) mice as black and gray bars, respectively (mean ± SEM). *, $P < 0.05$.

Fig. 2. Blood glucose and plasma insulin levels of the *RIP-C2mE* (*Tg*/–) mice loaded with glucose (glucose tolerance test). *A*, Blood glucose levels at 10, 20, 30, 60, 90 and 120 min after *i.p.* injection of glucose (1 g/kg body weight) in fasted mice. Data for the wild-type and *RIP-C2mE* (*Tg*/–) mice are indicated as black squares and gray triangles, respectively (mean ± SEM). *, $P < 0.05$ *versus* the wild-type level at the same age. *B*, Plasma insulin levels at 0 and 20 min after *i.p.* injection of glucose (1 g/kg body weight). Data for the wild-type and *RIP-C2mE* (*Tg*/–) mice are indicated in black and gray bars, respectively (mean ± SEM) *, $P < 0.05$.

Fig. 3. PGE_2 levels and chronological blood glucose in the *RIP-C2mE* (*Tg*/*Tg*) mice. *A*, The PGE_2 levels to the total pancreatic weight are indicated for the *RIP-C2mE* (*Tg*/−) mice and *RIP-C2mE* (*Tg*/ *Tg*) mice as black and gray bars, respectively (mean ± SEM). *B*, The relative islet PGE_2 levels are indicated for the *RIP-C2mE* (*Tg*/−) mice and *RIP-C2mE* (*Tg*/ *Tg*) mice as black bars and grey bars, respectively (mean ± SEM). *, $P < 0.05$. *C*, Chronological blood glucose levels in the wild-type mice (black squares), *RIP-C2mE* (*Tg*/−) mice (open triangles), and *RIP-C2mE* (*Tg*/*Tg*) mice (closed circles) at 3, 6, 9, and 12 weeks of age (mean ± SEM). *, $P < 0.05$ *versus* wild-type level at the same age.

Fig. 4. Fluorescence immunostaining of the islets for insulin (β-cell; green) and glucagon (α-cell; red) at 16 weeks of age. Representative results of two islets each for the wild-type mice (*A*), *RIP-C2mE* (*Tg*/−) mice (*B*), and *RIP-C2mE* (*Tg*/*Tg*) mice (*C*). Bars, 100 μm. The ratio of β-cells (*D*) and α-cells (*E*) to the total islet cells (mean ± SEM). *, $P < 0.05$.

Fig. 5. Fluorescence immunostaining of the pancreatic islets for insulin (β-cell; green) and glucagon (α-cell; red) at 3 weeks of age. Representative results for three islets each for the wild-type mice (*A*) and *RIP-C2mE* (*Tg*/*Tg*) mice (*B*). Bars in (*A* and *B*), 100 μm. The ratio of β-cells (*C*) and α-cells (*D*) to the total islet cells (mean ± SEM). Immunostaining for BrdU in the islets of the wild-type (*E*), *RIP-C2mE* (*Tg*/-) (*F*), and (*Tg*/*Tg*) (*G*) mice at 4 weeks of age. Arrowheads indicate BrdU-incorporated cells. Bars in (*E*-*G*), 50 μm. *H,* BrdU labeling index per islet of the respective mouse genotypes (mean ± SEM). *, $P < 0.05$.

Fig. 6. Representative histological analyses of the pancreatic islets of the *RIP-C2mE* (*Tg*/*Tg*) mice. *A*, Control islets from the wild-type mice (H & E). *B*, *RIP-C2mE* (*Tg*/*Tg*) mice (H&E). *C*, Immunostaining for the T cell marker CD3ε in the *RIP-C2mE* (*Tg*/*Tg*) mice. *D*, Immunostaining for the macrophage-specific F4/80 in the *RIP-C2mE* (*Tg*/*Tg*) mice. Arrows in (*A*-*D*) indicate islets. *E*, Fluorescent immunostaining for Gr-1 (green) and DAPI (blue) in the *RIP-C2mE* (*Tg*/*Tg*) mice. Arrow in (*E*) indicates Gr-1-positive neutrophil. *F*, The same section of (*E*) observed with a phase contrast microscope. Arrows in (*F*) indicate islets. Tissue sections were prepared from mice at 16 weeks of age (*A*-*D*) and 4 weeks of age (*E* and *F*). Bars, 100 μm.

Figure 1

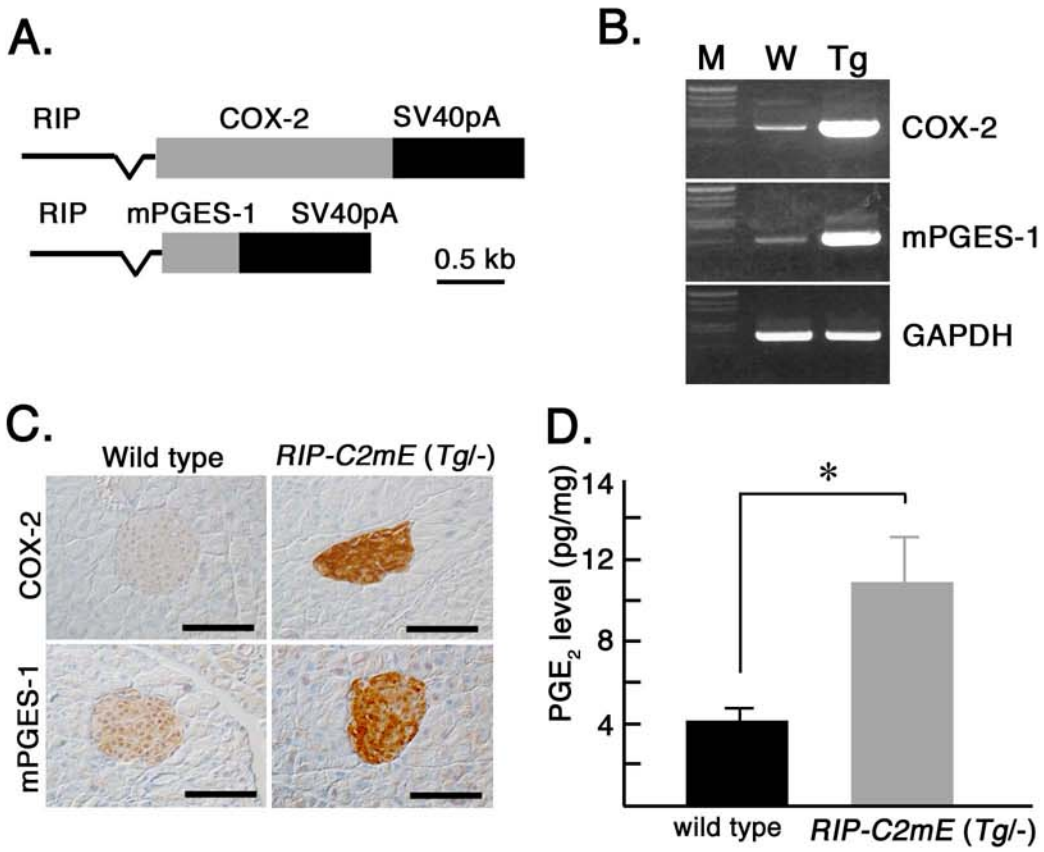
A.
RIP
COX-2
SV40pA
RIP
mPGES-1
SV40pA
0.5 kb
B.
M
W
Tg
COX-2
mPGES-1
GAPDH
C.
Wild type
RIP-C2mE (Tg/-)
COX-2
mPGES-1
D.
PGE2 level (pg/mg)
14
12
8
4
*
wild type
RIP-C2mE (Tg/-)

Figure 2

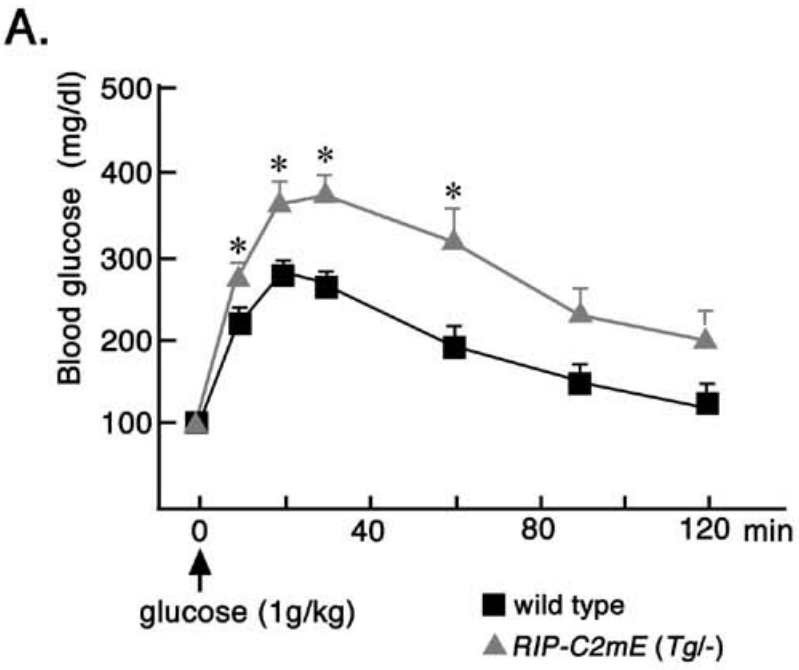
A.
Blood glucose (mg/dl)
500
400
300
200
100
0
40
80
120 min
glucose (1g/kg)
wild type
RIP-C2mE (Tg/-)

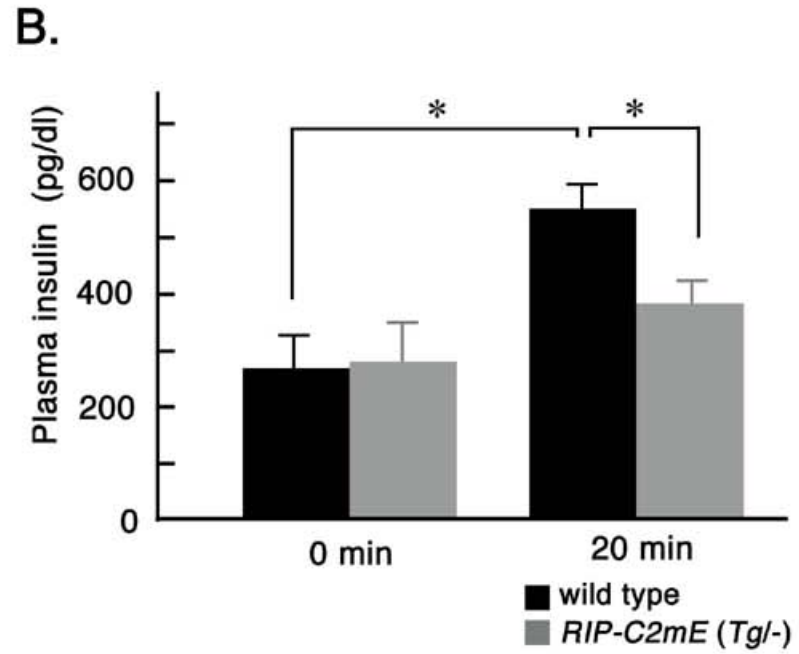
B.
Plasma insulin (pg/dl)
600
400
200
0
0 min
20 min
wild type
RIP-C2mE (Tg/-)

Figure 3

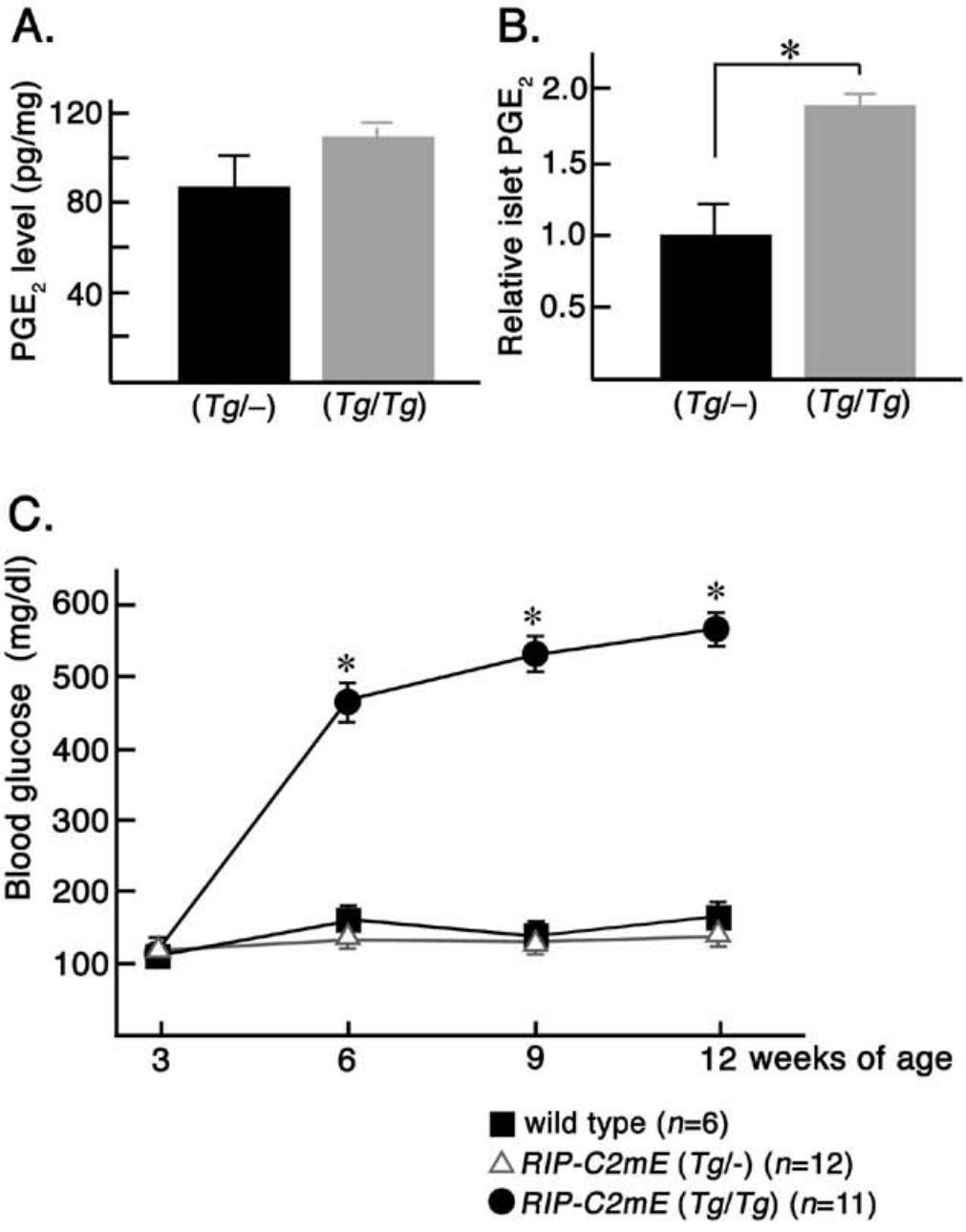
A.
PGE2 level (pg/mg)
120
80
40
(Tg/–)
(Tg/Tg)
B.
Relative islet PGE2
2.0
1.5
1.0
0.5
*
(Tg/–)
(Tg/Tg)
C.
Blood glucose (mg/dl)
600
500
400
300
200
100
*
*
*
3
6
9
12 weeks of age
wild type (n=6)
RIP-C2mE (Tg/-) (n=12)
RIP-C2mE (Tg/Tg) (n=11)

Figure 4

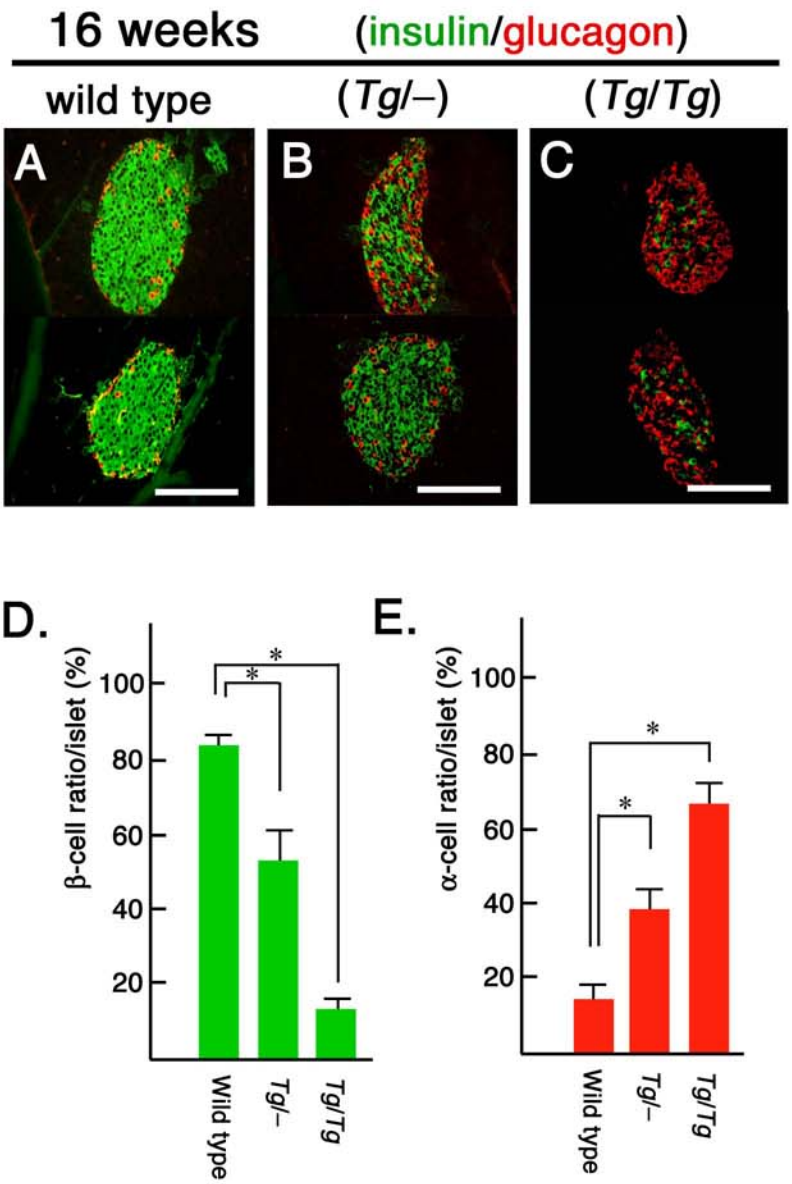
16 weeks
(insulin/glucagon)
wild type
(Tg/–)
(Tg/Tg)
A
B
C
D.
β-cell ratio/islet (%)
100
80
60
40
20
*
*
Wild type
Tg/–
Tg/Tg
E.
α-cell ratio/islet (%)
100
80
60
40
20
*
*
Wild type
Tg/–
Tg/Tg

Figure 5

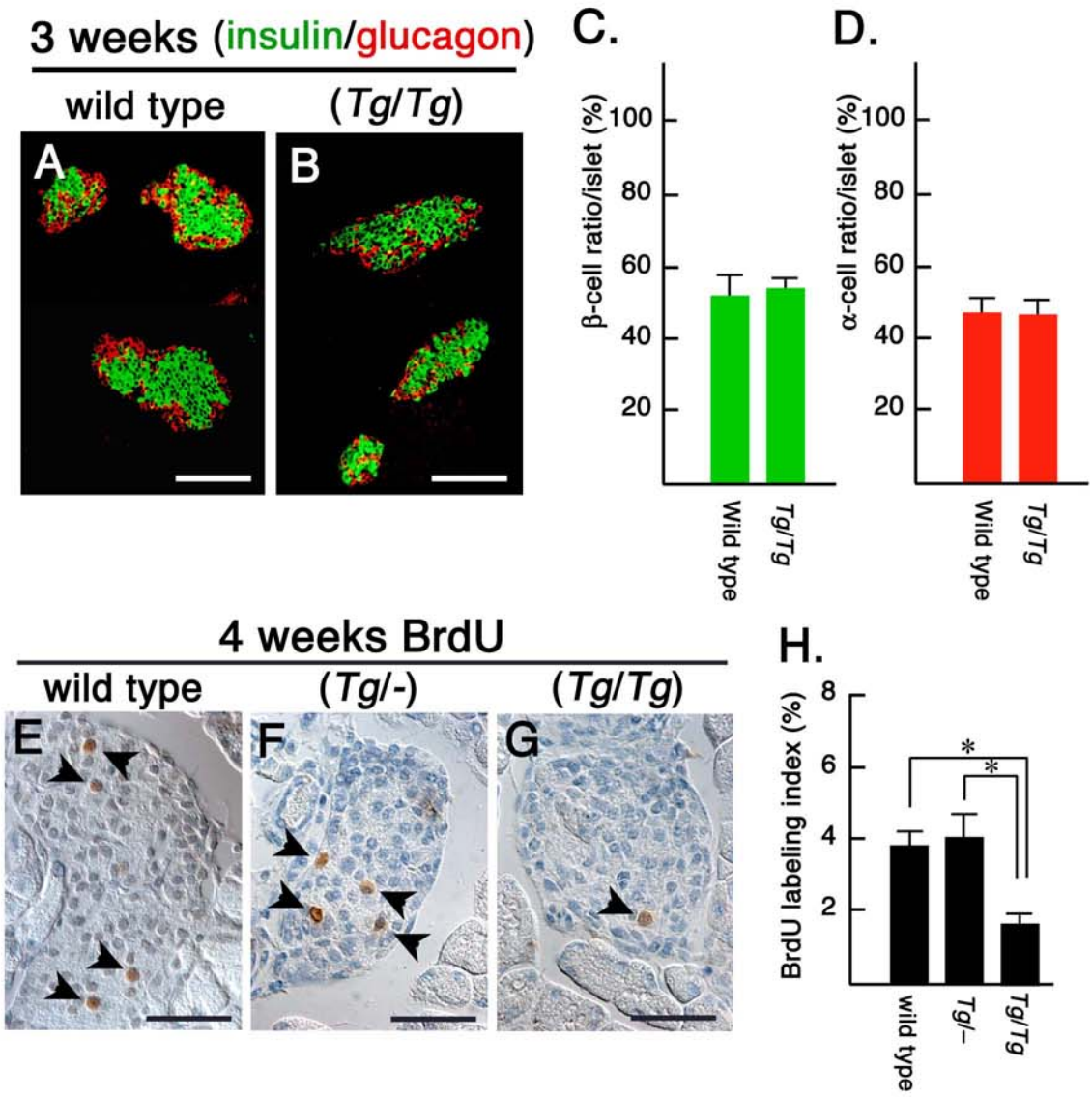
3 weeks (insulin/glucagon)
wild type
(Tg/Tg)
A
B
C.
β-cell ratio/islet (%)
100
80
60
40
20
Wild type
Tg/Tg
D.
α-cell ratio/islet (%)
100
80
60
40
20
Wild type
Tg/Tg
4 weeks BrdU
wild type
(Tg/-)
(Tg/Tg)
E
F
G
H.
BrdU labeling index (%)
8
6
4
2
*
*
wild type
Tg/–
Tg/Tg

Figure 6